

# Fast Human Activity Recognition based on Structure and Motion

Jinhui Hu and Nikolaos V. Boulgouris\*

*Department of Electronic Engineering, King's College, London, Strand, London WC2R 2LS, UK*

*Department of Electronic and Computer Engineering, Brunel University, Uxbridge, Middlesex UB8 3PH, UK*

---

## Abstract

In this paper, we present a method for the recognition of human activities. The proposed approach is based on the construction of a set of templates for each activity as well as on the measurement of the motion in each activity. Templates are designed so that they capture the structural and motion information that is most discriminative among activities. The direct motion measurements capture the amount of translational motion in each activity. The two features are fused at the recognition stage. Recognition is achieved in two steps by calculating the similarity between the templates and the motion features of the test and reference activities. The proposed methodology yields excellent results when applied on the INRIA database.

*Keywords:* Activity, recognition, surveillance

---

\*Corresponding author. Tel.: +44 1895 267629; fax: +44 1895 269782. E-mail address: nikolaos.boulgouris@brunel.ac.uk (N.V. Boulgouris).

## 1. Introduction

Although the earliest research in studying human movement was published in the 1850s [1], the automatic recognition of human activities [2], [3], [4], has emerged only recently as an important research area. The current research trend largely originated from a strong contemporary need for the development of applications, such as, automatic monitoring, surveillance, and intelligent human-computer interfaces. Human activity recognition is a very challenging task due to the great variability with which different people may perform the same activity.

Various approaches on activity representation and recognition have been presented during the past few years. One of the most important activity recognition techniques appeared in [5]. In that work, a motion template was introduced in order to describe a set of activities. Specifically, a binary motion-energy image (MEI) and a motion-history image (MHI) were introduced, which, when taken together, can be used as a two component version of a temporal template. Since its introduction, this approach has been widely used for the interpretation of human movement in image sequences.

The above approach was further improved in [6] in which temporal templates were extended to 3D in order to achieve viewpoint independence. The 2D silhouettes were extended to three dimensions (3D) using a visual hull [7]. Motion History Volumes (MHV) were introduced to represent human actions, which allow different camera configurations.

A popular group of approaches applied to human activity recognition use Hidden Markov Models (HMMs) [8], [9], [10], [11]. In [9], motion and shape features were represented using optical flow and eigen-shape vectors,

26 and HMMs were applied for recognition. An object trajectory-based activity  
27 recognition method using HMMs was introduced in [10], whereas in [11],  
28 several feature extraction algorithms based on PCA, ICA, and LDA, were  
29 applied and then followed by HMM modeling for recognition.

30 In [12], a method was proposed for human activity recognition based on  
31 an average template with a multiple-feature vector. The features that were  
32 used include the width feature as well as spatio-temporal features. Using the  
33 extracted features, Dynamic Time Warping (DTW) was used in combination  
34 with the average template to perform recognition.

35 In [13], activities were modeled based on their underlying dynamics and  
36 described as a cascade of dynamical systems. Further, methods were derived  
37 for the incorporation of view- and rate-invariance into the proposed models in  
38 order to enable similar activities to be directly clustered together regardless  
39 of view point or execution speed.

40 In [14], an example-based activity recognition was introduced by using  
41 an activity representation scheme according to which each activity was mod-  
42 eled as a series of synthetic poses. Recognition was achieved by matching  
43 the input silhouettes with the key poses using an enhanced Pyramid Match  
44 Kernel algorithm.

45 In [15], each activity was represented by descriptors using Temporal  
46 Laplacian Eigenmaps. Subsequently, all view-dependent manifolds were au-  
47 tomatically combined in order to find a representation in the 3D space that  
48 is independent from style and viewpoint. Dynamic time warping was applied  
49 for recognition.

50 In [16], an activity representation method was proposed which describes

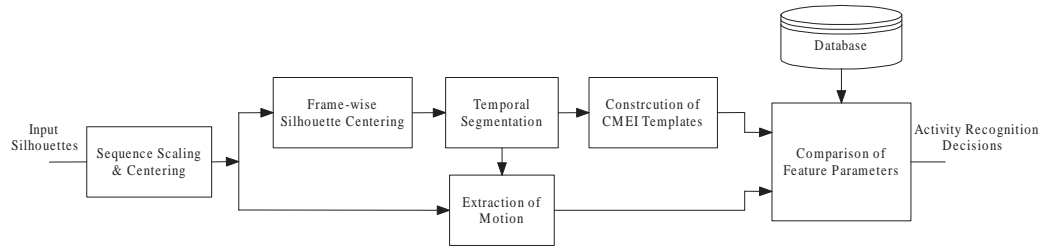
51 the video sequence using a set of spatiotemporal features called video-words.  
52 This was obtained by quantizing extracted 3D interest points. Then, the op-  
53 timal number of video-words clusters (VWCs) was determined by grouping  
54 the redundant video-words. Classification was achieved by using a correlo-  
55 gram.

56 The method we propose in this paper uses both shape-based and motion-  
57 based features, as the combination of these two types of features can improve  
58 the efficiency of the recognition process. Our approach is based on activity  
59 templates, which capture the information in the body postures assumed dur-  
60 ing each activity, as well as of the observed motion within each activity. After  
61 activity templates are constructed and the motion is calculated, recognition  
62 is achieved by means of comparison with the corresponding features that are  
63 stored in a database of reference activities.

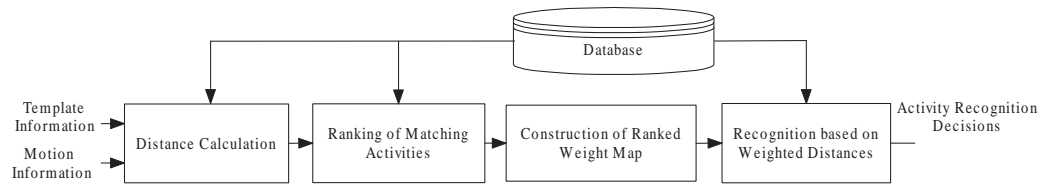
64 Recognition takes place in two stages. Initially, a number of best matches  
65 to the given test activity are calculated and, subsequently, the original selec-  
66 tion is refined by using a selection process that is tailored to discriminating  
67 among the best matches of the first recognition stage. Experimental results  
68 show that this approach is clearly more efficient than the direct recognition  
69 of a test activity among a diverse set of activities.

70 In summary, the contributions of the present paper are:

- 71 • A novel method for template construction based on centered silhou-  
72 ettes. We found that this construction is preferable to the conventional  
73 construction based on un-processed silhouettes.
- 74 • The representation of activities in terms of a spatiotemporal profile and  
75 a motion profile.



(a)



(b)

Figure 1: (a) General block diagram, (b) Detailed block diagram of the recognition process based on the motion and template information.

- 76 • A two-stage method for activity recognition based on discriminative  
77 weighting that is tailored to the best matching activities of a given test  
78 activity.

79 The structure of the paper is as follows: in Section 2, the proposed feature  
80 extraction methodology is described. In Section 3, two-phase activity recog-  
81 nition using discriminative weighting is presented. The proposed method  
82 is experimentally assessed for activity recognition in Section 4 and, finally,  
83 conclusions are drawn in Section 5.

## 84 **2. Feature Extraction For Recognition**

### 85 *2.1. Overview*

86 The proposed activity recognition system is outlined in Fig 1(a). The sys-  
87 tem operates under the assumption that the input to the system is sequences  
88 of binary silhouettes that depict the side-view of the person conducting the  
89 activity. In practice, however, there are cases in which the input sequences  
90 may not depict the side-view of the person. In the experimental results sec-  
91 tion, we investigate how this possible deviation from the assumed conditions  
92 affects the recognition performance of our system. Another assumption we  
93 are making is that activity segmentation from online video streams is per-  
94 formed using one of the existing approaches that are available in the litera-  
95 ture. Therefore, in this work we do not propose a new method for separating  
96 between consecutive activities in online video streams. Such an approach was  
97 presented in [17] in which temporal segmentation is based on the definition  
98 of motion boundaries, which is achieved through the computation of global  
99 motion energy.

100 After an initial scaling and centering stage, each activity sequence is tem-  
101 porally segmented into a number of parts, which define the stages in which  
102 the activity is performed. Considering the process of evolution of each activ-  
103 ity, we came to the conclusion that four stages suit the recognition best. The  
104 first and the last stages normally are the starting and ending poses and on  
105 many occasions (i.e., when the starting and ending pose is “standing”) they  
106 do not carry much discriminative information. The middle stages reflect the  
107 evolution of the activity. Having three stages in total, i.e., one middle stage  
108 only, would be insufficient. This means that at least four stages are needed

109 for discriminative representation and feature extraction. On the other hand,  
110 the maximum number of stages could potentially be five, as an even greater  
111 number of segments (e.g., six) could not capture further distinct poses in an  
112 activity. Therefore, the choice in our case was between having four and five  
113 stages. We found that using four stages is preferable both in terms of com-  
114 putational efficiency and performance, although the performance difference  
115 between using four and five stages is marginal.

116 Based on this temporal segmentation, motion and shape-based features  
117 are extracted from the input silhouette sequence. Specifically, for each of the  
118 four parts in a sequence, a template is constructed and a motion vector is  
119 calculated in order to quantitatively detect and represent translational mo-  
120 tion. The four motion vectors are subsequently combined with the activity  
121 templates at the decision stage in order to achieve efficient recognition. De-  
122 cisions are made by calculating the distance between the features extracted  
123 from a test activity and the features extracted from activities in the reference  
124 database. This process is outlined in Fig 1(b).

## 125 *2.2. Preprocessing*

126 In general, in a video sequence showing the performance of a given ac-  
127 tivity, the person performing the activity may be standing in an arbitrary  
128 position and have an arbitrary body pose. For this reason, prior to the cal-  
129 culation of the template, we scale and center the silhouettes. The scaling  
130 factor is obtained by calculating the ratio of the size of the foreground object  
131 in a standard frame over the object’s size in the first frame of each of the  
132 database sequences. This means that for each activity sequence there is a  
133 specific scale factor according to which all frames in this sequence are scaled.

Symbol	Notation
$i$	Frame index
$(x, y)$	Pixel co-ordinates
$F$	Total number of frames
$s$	Activity stage index
$a$	Activity index
$N$	Total number of activities
$\mathbf{T}_a$	Spatiotemporal profile for activity $a$
$\mathbf{t}_{as}$	sth stage template for activity $a$
$\mathbf{M}_a$	Motion profile for activity $a$
$\mathbf{m}_{as}$	sth stage motion profile for activity $a$
$\mathbf{R}_k$	$k$ th ranked spatiotemporal profile
$\mathbf{r}_{ks}$	sth stage template for ranked activity
$\mathbf{w}_s$	Weight map for stage $s$

Table 1: Notation

134 Centering of the foreground object, *i.e.*, of the person conducting the  
 135 activity, is applied after all silhouettes are scaled. Two kinds of centering  
 136 methods were tested: in the first method, horizontal displacements were  
 137 cancelled so that the foreground object is placed in the middle of the frame.  
 138 The same displacement vector was used for all frames in a sequence. In the  
 139 second method, silhouettes were centered on a frame by frame basis. The  
 140 averaged frames corresponding to these two different approaches are shown in  
 141 Fig 2. As seen, unlike the sequence-wise centering, the frame-wise centering  
 142 affects the vertical displacements during the activity.



Figure 2: Different centering approaches for the calculation of average images (sitting activity). (a) Sequence-wise centering, (b) Frame-wise centering.

143 *2.3. Temporal partitioning of activities*

144 An activity can be performed in dissimilar ways by different persons, or  
 145 even by the same person. One common difference is the speed with which  
 146 activities are executed. In practice, the speed with which a person is conduct-  
 147 ing an activity may vary even during the execution of the activity itself. The  
 148 great temporal variability in the way activities are performed necessitates the  
 149 deployment of methods that are robust to such variations. For this reason,  
 150 we partition each activity into activity stages and construct representative  
 151 pose templates for each such stage. To this end, we use a simple clustering  
 152 algorithm in order to effectively extract representative pose information. The  
 153 steps of the clustering process are summarized below:

- 154 1. Initially, an activity sequence with  $F$  frames is divided into four con-  
 155 tinuous temporal segments; each temporal segment has roughly  $F/4$   
 156 frames. Therefore, the initial temporal segment boundaries are:  $f_1 =$   
 157  $F/4, f_2 = F/2, f_3 = 3F/4, f_4 = F$ .

- 158 2. An average frame  $A_s, s = 1, \dots, 4$ , is calculated from each temporal  
 159 segment.
- 160 3. The sequence is partitioned into new temporal segments. Specifically,  
 161 new boundaries  $f'_s, s = 1, 2, 3, 4$ , are calculated between segments  $s$  and  
 162  $s + 1, s = 1, 2, 3$ , based on:

$$f'_s = \arg \min_f [D_s(f) + D_{s+1}(f)] \quad (1)$$

163 where  $D_s(f)$  and  $D_{s+1}(f)$  are the Euclidean distances between the  
 164 frames within each of the temporal segments and the segments cor-  
 165 responding average frame:

$$D_s(f) = \frac{1}{f - f_s + N} \sum_{i=f_s-N}^f D(I_i, A_s) \quad (2)$$

$$D_{s+1}(f) = \frac{1}{f_s + N - f + 1} \sum_{i=f}^{f_s+N} D(I_i, A_{s+1}) \quad (3)$$

- 167 4. Step 2 is repeated until convergence or until a maximum number of  
 168 iterations is reached.

169 Using the above simple technique, a given activity is divided into four  
 170 segments that correspond to four stages of the activity. A template can be  
 171 constructed for each stage. This construction is described next.

#### 172 2.4. Template Construction

173 We use two main features in our activity recognition algorithm. The first  
 174 is a spatiotemporal template that is mainly aimed to capture pose informa-  
 175 tion in human activities. The second feature is aimed to represent the motion  
 176 that is involved in the activity.

177 Motion Energy Images (MEI) and Motion History Images (MHI) were  
 178 proposed in [5] in order to encode, respectively, the location and the type of  
 179 motion. We propose the use of a similar temporal template in our system.  
 180 The similarity consists in the representation of the activity by means of  
 181 four MEI-like templates. In our case, however, the construction of the MEI  
 182 is based on a *centered* sequence of silhouettes. This approach makes the  
 183 impact of motion even more apparent on the resulting template, which we  
 184 will call *Centered MEI* (CMEI). Given an image sequence comprising frames  
 185  $I_j, j = 1, 2, \dots, F$ , the binary CMEI function is defined [5] as:

$$E_{\tau i} = \bigcup_{j=0}^{\tau-1} B_{t-j}(x, y) \quad (4)$$

186 where  $\tau$  is the duration of a movement. In our case, the value of  $\tau$  is set to  
 187 be the total number of frames in each stage of an activity execution. The  
 188 term  $B_j$  indicates the regions of motion according to the  $I_j$  and is calculated  
 189 using image-differencing:

$$B_j = C(I_{j+1}) - C(I_j) \quad (5)$$

190 where  $C(\cdot)$  denotes the centering operation.

191 Based on the above calculation, the template, corresponding to the  $a$ th  
 192 activity, will comprise of four *stage templates*  $\mathbf{t}_{as}, s = 1, \dots, 4$ . This repre-  
 193 sentation can be compactly expressed as:

$$\mathbf{T}_a = \{\mathbf{t}_{a1}, \mathbf{t}_{a2}, \mathbf{t}_{a3}, \mathbf{t}_{a4}\} \quad (6)$$

194 and, henceforth, it shall be referred to as *spatiotemporal profile*.

195 In Fig 3, the four stage templates are shown for each one of the twelve  
196 activities in the INRIA database. It can be seen that the resultant templates  
197 represent the information that *changes* throughout each activity, *i.e.*, the  
198 information that carries the most discrimination power. Due to their distinct  
199 characteristics, the four templates offer a compact activity representation of  
200 high discriminating capacity.

201 The above set of templates, based on the Motion Energy Image of an  
202 activity sequence, will be subsequently used for activity recognition purposes.  
203 As will be seen, despite its simplicity, this approach yields very good activity  
204 recognition performance.

### 205 *2.5. Extraction of Motion Information*

206 In our system, we take into consideration the amount of motion that  
207 takes place during the performance of an activity. As a measure of motion,  
208 in this case, we use the movement of the foreground object's center posi-  
209 tion. Unlike the template-based approach that was described previously, the  
210 method we propose for the extraction of motion is calculated based on the  
211 original sequence, without prior centering of the silhouettes, since any center-  
212 ing or scaling would affect the measured motion. This process is graphically  
213 illustrated in Fig 1(a).

214 In order to calculate the amount and the direction of motion, we consider  
215 the sequence of silhouette center coordinates  $(x_{ai}, y_{ai})$ ,  $i = 1, 2, \dots, F$ , for the  
216  $a$ th activity,  $a = 1, 2, \dots, N$ . Initially, the average center coordinate  $(\bar{x}_a, \bar{y}_a)$   
217 is calculated from this sequence. Therefore, for the  $a$ th activity, a sequence  
218 of difference vectors is initially formed:

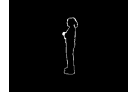
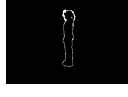
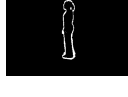
Activity	1	2	3	4
Check Watch				
Cross Arms				
Scratch Head				
Sit Down				
Get Up				
Turn Around & Walk				
Wave				
Punch				
Kick				
Point				
Pick Up				
Throw				

Figure 3: CMEI templates for each of the activities in the INRIA database.

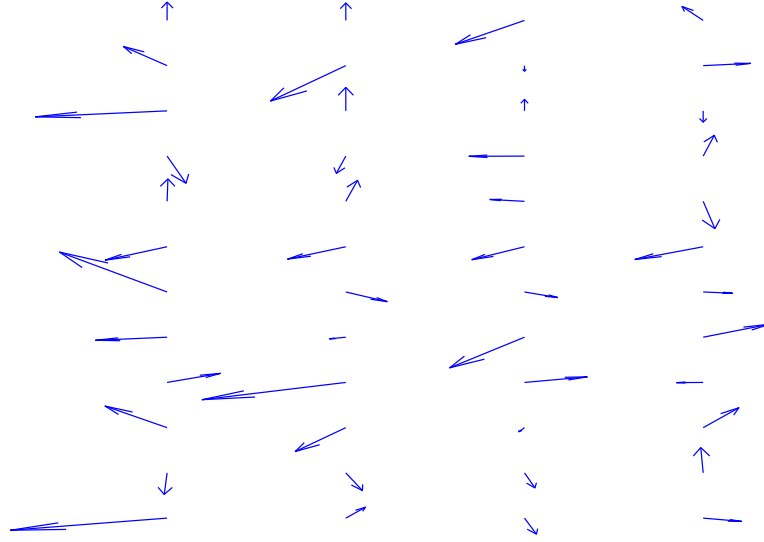


Figure 4: Graphical representation of motion profiles for each of the activities in the INRIA database. Each row of vectors represent a motion profile. The motion profile for the first activity is on the top row.

$$\mathbf{Z}_a(i) = \begin{bmatrix} x_{ai} - \bar{x}_a \\ y_{ai} - \bar{y}_a \end{bmatrix} \quad (7)$$

219 In the sequel, the motion for the  $a$ th activity is measured separately for  
 220 the four stages in each activity:

$$\mathbf{m}_{as} \triangleq \frac{1}{F_{as}} \sum_{i \in S_a} \mathbf{Z}_{as}(i), \quad s = 1, \dots, 4 \quad (8)$$

221 where  $F_{as}$  is the number of frames in activity  $a$  and  $S_a$  is the set of frame  
 222 indices in stage  $s$ . As seen, the above motion measurement essentially rep-  
 223 resents the translational motion of the center of the silhouettes with respect  
 224 to the average center of the foreground object for each stage of a particular  
 225 activity. Actually,  $\mathbf{m}_{as}$  corresponds to the silhouette center motion between  
 226 the first and the last frame of each stage. The contribution of such a feature  
 227 to a system's recognition efficiency may be small in cases where the person  
 228 performing the activity is standing or in case the person is engaging in an  
 229 activity with very limited motion. However, in cases where the person who  
 230 is conducting the activity is moving, this feature has a very considerable  
 231 contribution to recognition accuracy.

232 Based on the above, the motion information, corresponding to the  $a$ th  
 233 activity, will comprise of the four stage motion vectors  $\mathbf{m}_{as}, s = 1, 2, \dots, 4$ .  
 234 This can be compactly written as:

$$\mathbf{M}_a = \{\mathbf{m}_{a1}, \mathbf{m}_{a2}, \mathbf{m}_{a3}, \mathbf{m}_{a4}\} \quad (9)$$

235 and, henceforth, will be referred to as *motion profile*.

236 The four motion vectors for each of the 12 activities in the INRIA database  
 237 are shown in Fig 4. As seen, the motion profile of an activity includes a good  
 238 amount of discrimination power and, by itself, it could be used as a means for  
 239 recognition. Results using this type of information will be presented in the  
 240 experimental evaluation section. The above motion information will be used  
 241 in combination with the CMEI templates of the previous section in order to  
 242 achieve accurate recognition of activities.

### 243 **3. Two-phase Activity Recognition**

#### 244 *3.1. Distance Calculation*

245 Given a test sequence depicting an unknown activity, our objective is  
246 to recognize the activity that is being performed by comparison with a set  
247 of reference activities. Using our system, activity recognition is achieved  
248 by comparing the spatiotemporal and motion profiles of the unknown test  
249 activity to those of each of the reference activities. Recognition is achieved  
250 based on two types of extracted features, namely, the *CMEI templates in the*  
251 *spatiotemporal profiles* and the *activity motion profile*.

252 For the sake of description of our methodology, let us assume that a  
253 spatiotemporal profile  $\mathbf{T}_g$  is constructed from an unknown test activity se-  
254 quence. In order to recognize the index  $g$  of the unknown activity, distances  
255 are calculated between the profile obtained from the unknown test activity  
256 and the  $N$  activity profiles in a reference database. These distances, denoted  
257  $T_D$ , are compactly expressed as:

$$T_D[a] = d(\mathbf{T}_g, \mathbf{T}_a) \triangleq \sum_{s=1}^4 d(\mathbf{t}_{gs}, \mathbf{t}_{as}), \quad a = 1, 2, \dots, N \quad (10)$$

258 where  $d(\cdot)$  denotes the Euclidean distance, and  $\mathbf{T}_a$  is the profile constructed  
259 during the training session for the  $a$ th reference activity.

260 In a similar way, we can calculate the motion distance  $M_D$  between the  
261 motion profile  $\mathbf{M}_g$ , which was extracted from the test sequence, and the  $N$   
262 reference motion profiles that correspond to the  $N$  activities in the reference  
263 database:

$$M_D[a] = d(\mathbf{M}_g, \mathbf{M}_a) \triangleq \sum_{s=1}^4 d(\mathbf{m}_{gs}, \mathbf{m}_{as}), \quad a = 1, 2, \dots, N \quad (11)$$

264 Since it is reasonable to expect that  $T_D$  and  $M_D$  will have unequal con-  
 265 tributions to recognition performance, the total dissimilarity between a test  
 266 activity and the  $a$ th reference activity is defined as:

$$D[a] = T_D[a] + qM_D[a], \quad a = 1, 2, \dots, N \quad (12)$$

267 In the above definition,  $q$  is a parameter that is aimed to normalize the  
 268 contribution of the two distances during the calculation of the total distance.  
 269 The parameter  $q$  depends on the size of the foreground objects in the activity  
 270 video sequences and it is automatically readjusted whenever a change is made  
 271 in the scaling factor in the silhouette preprocessing stage. The value of  $q$  is  
 272 practically calculated as the value that equalizes the mean values of structural  
 273 distances and motion distances within the training set of activities.

274 In case there are several instances of each activity in the reference database,  
 275 then the distance  $D[a]$  in eq. (12) represents the distance between the test  
 276 activity and the instance of the  $a$ th activity in the database *that yields the*  
 277 *minimum distance.*

### 278 3.2. Discriminative Weighting

279 Considering that the issue of temporal variability of activities has been  
 280 addressed by our system with the extraction of four characteristic spatiotem-  
 281 poral templates, the main remaining obstacle in recognizing an activity cor-  
 282 rectly is the existence of different activities that look similar in the reference

283 database. The consequence of the above is that the variation between differ-  
 284 ent activities may appear to be smaller than the variation between different  
 285 instances of the same activity. Therefore, a given test activity may yield  
 286 a fairly small distance even when compared with a different activity in the  
 287 database.

288 One of the most popular ways to deal with problems like the above and  
 289 maximize recognition efficiency is by means of subspace projection using  
 290 Linear Discriminant Analysis (LDA) [18]. In such cases, the application of  
 291 LDA requires the conversion of images into long vectors that are subsequently  
 292 used for the calculation of eigenvectors and variance matrices. Since this  
 293 calculation can be difficult, the method in [19] is normally used in order to  
 294 make the problem computationally tractable. Unfortunately, the subspace  
 295 that can be obtained using this method is of dimension equal to the number  
 296 of classes. Since we only have a relatively small number of activities, the  
 297 resultant analysis would be quite restricting and would not generally give  
 298 good performance in the present scenario.

299 Another, much simpler, way to maximize recognition efficiency is by ap-  
 300 plying weighting that *highlights* the differences between activities during the  
 301 calculation of the distances. In this way, the template distance  $d(\mathbf{t}_{gs}, \mathbf{t}_{as})$  in  
 302 eq. (10) can be replaced by a weighted distance defined as:

$$\tilde{d}(\mathbf{t}_{gs}, \mathbf{t}_{as}) \triangleq \sum_x \sum_y \tilde{\mathbf{w}}(x, y) |\mathbf{t}_{gs}(x, y) - \mathbf{t}_{as}(x, y)|, \quad s = 1, \dots, 4 \quad (13)$$

303 where  $\tilde{\mathbf{w}}(x, y)$  is the weighting coefficient at template position  $(x, y)$ . The  
 304 weighting coefficients should be greater in template areas that differ among

305 different activities and smaller coefficients in areas of similarity. Conse-  
306 quently, if we attempt to design a weight map in order to optimally dis-  
307 tinguish among different activities, the distribution of energy on the weight  
308 map will be primarily dependent on activities that are very dissimilar. On  
309 the contrary, similar activities will make smaller contributions to the weight  
310 map. Clearly, a weight map calculated as above will be inefficient for dis-  
311 tinguishing between activities with small differences. Therefore, the problem  
312 of distinguishing between similar activities cannot be dealt with using the  
313 above straightforward weight map design.

314 In order to overcome this problem, we propose using a two-phase ap-  
315 proach in which, once all distances are calculated as above, the activities are  
316 first ranked in order of increasing distance. Subsequently, the  $K$  reference  
317 activities that rank higher, *i.e.* those that exhibit the greatest similarity with  
318 the test activity, are used for the design of a weight map that is aimed to  
319 facilitate discrimination among these  $K$  activities. Apparently, we need the  
320 actual matching reference activity to always be among the  $K$  best matches  
321 in order to be able to recognize the test activity in the second phase of the  
322 classification process. However, the greater  $K$  is, the lower the efficiency of  
323 the weighted approach will be. In this work, we use  $K = N/3 = 4$ , as it was  
324 found that this choice represents a good compromise between recognition  
325 efficiency in the two phases of the algorithm. The impact of choice of  $K$  in  
326 the first phase of the algorithm is shown in Table 2. As seen, in the vast  
327 majority of cases, the actual matching reference activity is among the four  
328 best matches.

329 The weight map calculated based on the  $K$  highest ranking activities is

	Rank							
Act No.	1	2	3	4	5	6	7	8
1	72	83	97	100	100	100	100	100
2	83	95	100	100	100	100	100	100
3	87	100	100	100	100	100	100	100
4	98	100	100	100	100	100	100	100
5	100	100	100	100	100	100	100	100
6	100	100	100	100	100	100	100	100
7	83	97	100	100	100	100	100	100
8	37	53	62	85	98	100	100	100
9	82	87	95	100	100	100	100	100
10	35	57	78	88	100	100	100	100
11	73	87	93	100	100	100	100	100
12	58	60	63	87	92	100	100	100

Table 2: Cumulative match scores for the performance (in percent) of the first phase of the classification algorithm.

330 now tailored to the task of distinguishing between activities that, despite  
331 being different, they look similar to the test activity. This approach is ex-  
332 pected to be more efficient than discrimination techniques that are based on  
333 all activities in the database.

334 For the calculation of the weight map, we denote the spatiotemporal  
335 profile of the  $k$ th ranked reference activity as:

$$\mathbf{R}_k = \{\mathbf{r}_{k1}, \mathbf{r}_{k2}, \mathbf{r}_{k3}, \mathbf{r}_{k4}\}, \quad k = 1, 2, \dots, K \quad (14)$$

336 In the above expression,  $k$  is index of the the ranked reference activities,  
 337 *i.e.*,  $\mathbf{R}_1$  is the spatiotemporal profile of the reference activity that exhibits  
 338 the smallest distance with the test activity,  $\mathbf{R}_2$  exhibits the second smallest  
 339 such distance and so on. We calculate the weight map based on the profile  
 340 coefficients that appear to contribute to the discrimination among the  $K$   
 341 ranked profiles  $\mathbf{R}_{ks}, k = 1, 2, \dots, K$ , that correspond to the activities that  
 342 are most similar to the test activity.

343 We define the total “*between*” difference  $\mathbf{v}_s^B(x, y)$  in pixel position  $(x, y)$   
 344 between *different* ranked activities as:

$$\mathbf{v}_{Bs}(x, y) = \frac{1}{K^2} \sum_{k=1}^K \sum_{l=1}^K |\mathbf{r}_{ks}(x, y) - \mathbf{r}_{ls}(x, y)|, \quad s = 1, \dots, 4 \quad (15)$$

345 As seen, a separate difference matrix is calculated for each activity stage  
 346  $s$ . Considering the symmetricity of the template differences in eq. (15), the  
 347 above expression can be equivalently written as:

$$\mathbf{v}_{Bs}(x, y) = \frac{1}{K^2} \sum_{k=1}^{K-1} \sum_{l=k+1}^K 2|\mathbf{r}_{ks}(x, y) - \mathbf{r}_{ls}(x, y)|, \quad s = 1, \dots, 4 \quad (16)$$

348 Subsequently, for the  $K$  ranked activities, we calculate a total “*within*”  
 349 difference matrix using  $H$  different instances of the *same* activity:

$$\mathbf{v}_s(i, j) = \frac{1}{KH^2} \sum_{k=1}^K \left( \sum_{b=1}^{H-1} \sum_{c=b+1}^H 2|\mathbf{r}_{ks}^b(x, y) - \mathbf{r}_{ks}^c(x, y)| \right), \quad s = 1, \dots, 4 \quad (17)$$



Figure 5: Weight map for a set of best matches comprising of activities: *check watch*, *cross arms*, *scratch head*, and *wave*.

350 In a way that is reminiscent of Linear Discriminant Analysis, when apply-  
 351 ing eq. (13), we can emphasize “between” differences and suppress “within”  
 352 differences by using weighting coefficients calculated based on the ratio of eq.  
 353 (16) and (17). Specifically, the elements  $\mathbf{w}_s(x, y)$  of the weight map can be  
 354 calculated as:

$$\mathbf{w}_s(x, y) = \frac{\mathbf{v}_{B_s}(x, y)}{L + \mathbf{v}_s(x, y)}, \quad s = 1, \dots, 4 \quad (18)$$

355 where  $L$  is a small number that is aimed to prevent the denominator of the  
 356 right-hand side from becoming zero (in our experiments we used  $L = 0.5$ ).

357 A weight map determined based on four activities: *check watch*, *cross*  
 358 *arms*, *scratch head*, and *wave*, is shown in Fig 5. As can be seen, despite the  
 359 fact that the differences between these activities are very subtle, recognition  
 360 is facilitated by focusing the recognition process on exactly these differences.  
 361 This performance would not have been possible if the weight map calculation  
 362 had been based on all activities in the database.

363 *3.3. Recognition*

364 Once the weight map has been determined, weighted template distances  
365 are calculated between the test activity and the reference activity templates.

366 The weighted template distance is defined as:

$$\tilde{T}_D[a] = \tilde{d}(\mathbf{T}_g, \mathbf{T}_a) \triangleq \sum_{s=1}^4 \tilde{d}(\mathbf{t}_{gs} - \mathbf{t}_{as}) \quad (19)$$

367 and the associated total weighted distance is:

$$\tilde{D}[a] = \tilde{T}_D[a] + qM_D[a], \quad a = 1, 2, \dots, N \quad (20)$$

368 where the value of the parameter  $q$  is selected according to the process de-  
369 scribed in the beginning of this section.

370 The system recognizes the test activity based on the minimum total  
371 weighted distance among all results:

$$G = \arg \min_a \tilde{D}[a] \quad (21)$$

372 where  $G$  is the index of the recognized activity.

373 **4. Experimental Results**

374 In order to evaluate the performance of our system, we tested the pro-  
375 posed algorithm on the INRIA Xmas Motion Acquisition Sequences (IXMAS)  
376 Database [6]. The INRIA multi-view database includes 12 daily-life activi-  
377 ties each performed 3 times by 12 actors. Surrounded with 5 fixed cameras,  
378 each capturing 23 frames per second, the actors freely choose their position

379 and orientation while they perform the activities. All 12 activities are per-  
380 formed in the same order, but with a different execution rate, depending on  
381 the actors. For the evaluation of our method, we used 72 sequences, *i.e.*, 72  
382 different instances of each activity. Therefore, we used 864 ( $72 \times 12$ ) activity  
383 executions in total.

384 In our experiments, we used views “1” and “2” from the INRIA database  
385 which are different as they are captured using different cameras. For the  
386 construction of the *reference* (*i.e.*, training) spatiotemporal profiles and the  
387 extraction of the *reference* motion profiles, we used twelve activity sequences,  
388 which were chosen randomly from these two views (six from each). Each of  
389 these reference sequences contained all 12 activities. This means that 144  
390 ( $12 \times 12$ ) activity executions were used for training. The remaining 720  
391 ( $60 \times 12$ ) activity executions were used as test sequences.

392 Initially, we applied our baseline method, using template and motion in-  
393 formation, without applying any weighting on the spatiotemporal profiles.  
394 The first three columns of Table 3 report results based on the independent  
395 application of the motion profile, the spatiotemporal *Centered MEI profile*  
396 (CMEI), as well as their combination (CMM). As seen, the performance of  
397 these features when used independently is not always good. However, if they  
398 are combined using eq. (20), then the resulting method, termed *Centered*  
399 *MEI with Motion* (CMM), exhibits apparent performance improvements, es-  
400 pecially if compared with the independent use of the motion feature.

401 Subsequently, we applied the two-phase process described in Section 3.  
402 The four best matches for each given test activity were calculated and a  
403 weight map was designed in order to facilitate recognition among these four

No.	Action	Motion	Baseline		Weighted	
			CMEI	CMM	wCMEI	wCMM
1	Check Watch	61.67	70.00	71.67	88.33	<b>91.67</b>
2	Cross Arms	45.00	76.67	83.33	86.67	<b>90.00</b>
3	Scratch Head	46.67	83.33	86.67	81.67	<b>88.33</b>
4	Sit Down	<b>100</b>	96.67	98.33	98.33	98.33
5	Get Up	<b>100</b>	<b>100</b>	<b>100</b>	<b>100</b>	<b>100</b>
6	Turn & Walk	<b>100</b>	98.33	<b>100</b>	<b>100</b>	<b>100</b>
7	Wave	33.33	81.67	83.33	83.33	<b>85.00</b>
8	Punch	21.67	36.67	36.67	<b>68.33</b>	<b>68.33</b>
9	Kick	31.67	81.67	81.67	85.00	<b>86.67</b>
10	Point	43.33	33.33	35.00	61.67	<b>63.33</b>
11	Pick up	76.67	68.33	73.33	80.00	<b>81.67</b>
12	Throw	31.67	56.67	58.33	71.67	<b>76.67</b>
Average		57.64	73.61	75.69	83.75	<b>85.83</b>

Table 3: Activity recognition rates by using motion profiles, CMEI templates, combined CMM profiles, and discriminate weighting.

404 matches. Results are reported in the last two columns of Table 3 for the  
405 weighted CMEI (wCMEI) profile, and the combined *weighted CMEI with*  
406 *motion*, termed wCMM. As seen, the recognition rate is very considerably  
407 improved when compared with the un-weighted CMM method. Despite its  
408 simplicity, the combination of the motion profile with the weighted spatiotem-  
409 poral profile yields excellent performance. Using our current system, the test  
410 activity sequences are recognized correctly at an average recognition rate of

No.	Action	1	2	3	4	5	6	7	8	9	10	11	12
1	Check Watch	91.7	3.3	3.3	0	0	0	1.7	0	0	0	0	0
2	Cross Arm	5.0	90.0	3.3	0	0	0	1.7	0	0	0	0	0
3	Scratch Head	5.0	3.3	88.3	0	0	0	3.3	0	0	0	0	0
4	Sit Down	0	0	0	98.3	0	0	0	0	0	0	1.7	0
5	Get Up	0	0	0	0	100	0	0	0	0	0	0	0
6	Turn & Walk	0	0	0	0	0	100	0	0	0	0	0	0
7	Wave	3.3	1.7	6.7	0	0	0	85.0	0	0	1.7	0	1.7
8	Punch	6.7	0	8.3	0	0	0	5	68.3	0	10	0	1.7
9	Kick	0	1.7	0	1.7	0	0	0	3.3	86.7	1.7	1.7	3.3
10	Point	3.3	8.3	5	0	0	0	3.3	13.3	0	63.3	0	3.3
11	Pick Up	0	0	0	8.3	3.3	0	0	1.7	3.3	0	81.7	1.7
12	Throw	5	0	1.7	0	0	0	10	3.3	0	3.3	0	76.7

Table 4: Confusion Matrix of our final system on the INRIA Database.

411 85.83%, which constitutes a significant improvement on the performance of  
 412 the baseline system. As will be discussed later, this performance also consti-  
 413 tutes an improvement over other recently published methods, such as those  
 414 in [14], [15], [16]. The confusion matrix reporting confusion between activi-  
 415 ties recognized by the proposed wCMM system is shown in Table 4. Table  
 416 4 shows that the system is occasionally prone to confuse the “point” and  
 417 the “punch” activity, which is consistent with the results presented in Table  
 418 3. The less satisfactory performance on these two activities is due to their  
 419 inherent similarity as well as the great variability with which subjects are  
 420 performing the “punch” and “point” activities in the testing set that we use

No.	Action	inter	intra
1	Check Watch	88.33	93.33
2	Cross Arms	90.00	91.67
3	Scratch Head	86.67	91.67
4	Sit Down	98.33	98.33
5	Get Up	100	100
6	Turn & Walk	100	100
7	Wave	83.33	88.33
8	Punch	58.33	68.33
9	Kick	80.00	85.00
10	Point	63.33	63.33
11	Pick up	81.67	81.67
12	Throw	73.33	76.67
Average		83.61	86.53

Table 5: Evaluation of the proposed wCMM method under viewpoint variations.

421 for our experiments.

422 In order to test the performance of our system under viewpoint variation,  
423 two views with moderate differences are chosen. We report results in two  
424 forms, first we use different views for training and testing, and then we train  
425 and test using activity sequences from the same view. The results are shown  
426 in Table 5. As seen, although there is a decrease in recognition performance  
427 in the cross-view experiment, the decrease is not dramatic and demonstrates  
428 that our system can work well even when the actual view is different from  
429 the assumed one.

430 Finally, we compared our wCMM method with a variety of other existing  
431 techniques for activity recognition. Specifically, the other methods in our  
432 comparison are the Action Net method [14], the Action Manifolds [15], as  
433 well as the method in [16]. The recognition performance of our system in  
434 comparison to the recognition performance of other approaches is shown in  
435 Table. 6. As seen, our wCMM method outperforms the other methods in  
436 the comparison for activity recognition, which reinforces our confidence about  
437 the advantages that our approach offers.

Method	wCMM	Action Net [14]	Action Manifolds [15]		VWCs [16]
View	single	multiple	multiple	single	multiple
Recognition Rate	<b>85.83</b>	80.6	83.1	80.3	78.5

Table 6: Comparison of our proposed method in comparison to other competing methods in terms of average recognition performance.

## 438 5. Conclusion

439 In this paper, we presented a method for the recognition of human activ-  
440 ities. The proposed approach was based on the construction of a set of tem-  
441 plates for each activity as well as on the measurement of the motion in each  
442 activity. Templates were designed so that they capture the structural and  
443 motion information that is most discriminative among activities. The direct  
444 motion measurements capture the amount of translational motion in each  
445 activity. The two features are fused at the recognition stage. Recognition  
446 is achieved in two steps by calculating the similarity between the templates

447 and the motion features of the test and reference activities. The proposed  
448 methodology yielded excellent results when applied on the INRIA database.

## 449 **6. Acknowledgements**

450 This work was supported in part by the European Commission under  
451 Contract FP7-215372 ACTIBIO

452 The authors would like to thank the anonymous reviewers for their careful  
453 and constructive review, which resulted in a greatly improved manuscript.

- 454 [1] E. Muybridge, *The Human Figure in Motion*, Dover Publications, 1901.
- 455 [2] J. K. Aggarwal, Q. Cai, Human motion analysis: A review, *Computer*  
456 *vision and image understanding* 73 (3) (1999) 428–440.
- 457 [3] D. M. Gavrila, The visual analysis of human movement: a survey, *Com-*  
458 *puter vision and image understanding* 73 (1) (1999) 82–98.
- 459 [4] W. Liang, H. Weiming, T. Tan, Recent developments in human motion  
460 analysis, *Pattern Recognition* 36 (3) (2003) 585–601.
- 461 [5] A. F. Bobick, J. W. Davis, The recognition of human movement us-  
462 ing temporal templates, *IEEE Tran. on Pattern Analysis and Machine*  
463 *Intelligence* 23 (3) (2001) 257–267.
- 464 [6] D. Weinland, R. Ronfard, E. Boyer, Free viewpoint action recognition  
465 using motion history volumes, *Computer vision and image understand-*  
466 *ing* 104 (2-3) (2006) 249–257.

- 467 [7] A. Laurentini, The visual hull concept for silhouette-based image under-  
468 standing, *IEEE Tran. on Pattern Analysis and Machine Intelligence* 16  
469 (1994) 150–162.
- 470 [8] M. Piccardi, O. Perez, Hidden markov models with kernel density es-  
471 timation of emission probabilities and their use in activity recognition,  
472 in: *IEEE Computer Society Conf. on Computer Vision and Pattern*  
473 *Recognition*, Minnesota, US, 2007, pp. 1–8.
- 474 [9] F. Niu, M. A. Mottaleb, Hmm-based segmentation and recognition of  
475 human activities from video sequences, in: *IEEE Int. Conf. on Multi-*  
476 *media and Expo*, Amsterdam, Netherlands, 2005, pp. 804–807.
- 477 [10] F. I. Bashir, A. A. Khokhar, D. Schonfeld, Object trajectory-based ac-  
478 tivity classification and recognition using hidden markov models, in:  
479 *IEEE Tran. on Image Processing*, 2007, pp. 1912 – 1919.
- 480 [11] J. J. L. Md. Zia Uddin, T. S. Kim, Independent component feature-  
481 based human activity recognition via linear discriminant analysis and  
482 hidden markov model, in: *IEEE EMBS Conf.*, 2008, pp. 5168–5171.
- 483 [12] S. Cherla, K. Kulkarni, A.Kale, V. Ramasubramanian, Towards fast,  
484 view-invariant human action recognition, in: *IEEE Conf. on Computer*  
485 *Vision and Pattern Recognition Workshops*, 2008, pp. 1–8.
- 486 [13] P. Turaga, A. Veeraraghavan, R. Chellappa, Unsupervised view and  
487 rate invariant clustering of video sequences, *Computer vision and image*  
488 *understanding* 113 (2009) 353–371.

- 489 [14] F. Lv, R. Nevatia, Single view human action recognition using key pose  
490 matching and viterbi path searching, *Computer Vision and Pattern*  
491 *Recognition CVPR 2007 2008* (2007) 1–8.
- 492 [15] M. Lewandowski, D. Makris, J. Nebel, View and style-independent ac-  
493 tion manifolds for human activity recognition, *Computer vision* 6316  
494 (2010) 547–560.
- 495 [16] J. Liu, S. Ali, M. Shah, Recognizing human actions using multiple  
496 features, *Computer Vision and Pattern Recognition CVPR 2008 2008*  
497 (2008) 1–8.
- 498 [17] D. Weinland, R. Ronfard, E. Boyer, Automatic discovery of action tax-  
499 onomies from multiple views, in: *IEEE Computer Society Conf. on Com-*  
500 *puter Vision and Pattern Recognition*, 2006, pp. 1639 – 1645.
- 501 [18] P. H. R.O. Duda, D. Stork, *Pattern Classification*, John Wiley & Sons,  
502 Inc., 2001.
- 503 [19] M. Turk, A. Pentland, Face recognition using eigenfaces, in: *Conf. on*  
504 *Computer Vision and Pattern Recognition*, 1991.